Journal of Renewable Materials

Tech Science Press

DOI: 10.32604/jrm.2023.027160

ARTICLE

Surfactant-Modified Hydrophobic Biochar Derived from Laver (*Porphyra haitanensis*) with Superior Removal Performance for Kitchen Oil

Jiaxing Sun[1], Lili Ji[1,*], Qianrui He[1], Ran Li[1], Xiaoyue Xia[2], Yaning Wang[1], Yi Yang[2], Lu Cai[3] and Jian Guo[2]

[1]National Marine Facilities Aquaculture Engineering Technology Research Center, Zhejiang Ocean University, Zhoushan, 316022, China

[2]College of Food and Medical, Zhejiang Ocean University, Zhoushan, 316022, China

[3]Institute of Ocean Higher Education, Zhejiang Ocean University, Zhoushan, 316022, China

[*]Corresponding Author: Lili Ji. Email: jll-gb@163.com

Received: 17 October 2022 Accepted: 01 December 2022 Published: 26 June 2023

ABSTRACT

In this study, a novel absorpent (MSAR600°C) with a hydrophobic surface and hierarchical porous structure for the removal of kitchen oil was facilely fabricated from the macroalgae, laver (*Porphyra haitanensis*) by incorporating high-temperature carbonization and alkyl polyglucosides (APG) and rhamnolipid (RL) surfactants modification. The characterization results showed MSAR600°C possessed a louts-leaf-like papillae microstructure with high contact angle (137.5°), abundant porous structure with high specific surface area (23.4 m^2/g), and various oxygen-containing functional groups (-OH, C=O, C-O). Batch adsorption experiments were conducted to investigate the effect of adsorption time, temperature, pH, and absorbent dose on kitchen oil adsorption performance. Then the practical application for the removal of kitchen oil using MSAR600°C was also performed. The results showed that MSAR600°C had a higher removal efficiency for kitchen oil (75.98%), compared with the commercial detergent (72.3%). This study demonstrates an example of fabricating a green tableware detergent for enhanced removal performance of kitchen oil.

KEYWORDS

Laver biochar; surfactant modification; kitchen oil; removal mechanism

1 Introduction

Tableware detergent, also known as dishwashing essence, mainly consists of solvent (generally deionized water), surfactant, pH regulator, thickener, substance, preservative, pigment, etc. [1–3]. The above components are chemical agents; after use, large quantities of ingredients are released into the aquatic and terrestrial environments, which pose a threat to human health and the ecological environment. Considering the disadvantages of traditional tableware detergents, natural, ecological, and sustainable detergents are on their way coming into the market.

As is well known, kitchen oil is one oily wastewater. Various technologies have been developed for the treatment of oily wastewater, including absorption, membrane separation, centrifugation separation, biological therapy, air floatation, etc. [4], among which, adsorption is one of the most widely applied

technologies due to its high efficiency, easy to operate and cost-effective [5]. It has been found that natural biomass sorbents are the most readily biodegradable, low-cost, and easily available sorbents, whose adsorption efficiency can be enhanced significantly by activation and or carbonization [6,7]. Biochar is a material produced from natural biomass by activation or/and carbonization in the absence of limited oxygen conditions [8]. Recently, biochar has been studied widely in heavy metals and organic contaminants removal, soil remediation, as well as supercapacitor [9–11]. At the same time, in oily wastewater treatment, there is a relatively small percentage, mainly focusing on the removal of diesel [12] and crude oil [13]. The main reason is that the surface of biochar is hydrophilic due to its abundant hydroxyl groups. According to the principle of similarity and intermiscibility, the oil removal efficiency of biochar is not good.

According to the Young equation, Cassie wettability model, and Wenzel wettability model, the main factors affecting the wettability of a solid surface are its surface free energy and microstructure [14]. To obtain specific wettability, it has been developed and designed a variety of methods to improve the surface wettability of solid materials, such as introducing hydrophilic or hydrophobic groups [15], surface treatment [16], coating [17], formation of porous structures or surface defects [18,19]. Adding hydrophilic or hydrophobic groups or surface coating can change the surface energy to obtain controllable wettability. Modifying surface structure by properly designing a porous structure or creating defects is another effective method to regulate wettability. The oil removal efficiencies of biochar mainly depend on its surface hydrophobicity; thus we could modify the surface of biochar to enhance the adsorption performance of oil [20]. Lauric Acid (LA), a surfactant, can increase biochar hydrophobicity and water contact angle by decorating biochar surface, which gives higher oil adsorption capacities [21–23]. In our previous studies, we applied surfactants to modify calcined mussel shell powder (CMSP) to remove oil. First, alkyl polyglucosides (APG) and dimethyl octadecyl hydroxy ethyl ammonium nitrate (SN) were applied to modify the surface of CMSP, endowing the functions of emulsifying oil and diverting net charge. The detergency rate of oil increased to 17.35% [24]. Moreover, we also used alkyl polyglucosides (APG) and rhamnolipid (RL) to modify CMSP, rendering CMSP a lipophilic surface, and its removal rate from kitchen oil reached 87.05% [25]. Therefore, the surface hydrophobicity of biochar can be regulated by a surfactant to improve the adsorption capacity of oily wastewater.

Recently, algae, with high biomass and short growth cycle compared to terrestrial plants has been considered a new raw material for the preparation of biochar [26]. Laver, a red alga, has a wide breeding area in China. However, the high-value utilization of laver is still low, restricting the development of the laver industry. Recently, laver biochar has attracted considerable attention due to its excellent adsorption performance, more accessible, and low price [27–29]. However, the potential for kitchen oil removal of algae biochar has not yet been studied. Thus, in this work, a novel tableware detergent for the removal of kitchen oil was designed and prepared by using alkyl polyglucosides (APG) and rhamnolipid (RL) to modify biochar derived from laver through a two-step hydrothermal synthesis method, endowing it hydrophobic surface properties. The hydrophobic properties, pore morphology, crystal phase composition, functional groups, and chemical valence state of the as-prepared composite materials were characterized. And then, the removal performance of kitchen oil using the as-prepared samples was analyzed.

2 Materials and Methods

2.1 Materials and Chemicals

Dry laver (*Porphyra haitanensis*) was purchased from Rudong Shunfa Laver Products Co., Ltd. in Jiangsu Province, China. Alkyl glycosides (APG, APG2000, 8~10 carbon alkyl chain) and rhamnolipid (RL, 98%) were purchased from Shanghai Fine Chemicals Co., Ltd., China). Commercial tableware detergent (CAD Guangzhou Libai Group Co., Ltd., China). and kitchen oil (Golden Arowana Grain, Oil

and Food Co., Ltd., Zhoushan, China) were purchased from the supermarket in Zhoushan, Zhejiang Province, China. All the chemical reagents used in this experiment were analytical grade.

2.2 Preparation of Laver Biochar

Dry laver was soaked in distilled water for 24 h, rinsed repeatedly with distilled water, dried in an oven at 80°C for 24 h, and crushed for the pyrolysis experiment. Laver powder was placed in a tube furnace, heated to the pyrolysis temperature at a rate of 10 °C/min under an N_2 atmosphere with a flow rate of 100 mL/min, and kept at the pyrolysis temperature for 2 h. The pyrolysis temperatures of laver were set to 500°C, 600°C, 700°C and 800°C, respectively. After pyrolysis, the cooling rate was set to 10 °C/min. When the temperature dropped to 500°C, the furnace was cooled naturally. The obtained laver biochar was ground to pass through a 100-mesh sieve. The as-prepared laver biochar calcined at 500°C, 600°C, 700°C and 800°C were denoted as CSB500°C, CSB600°C, CSB700°C and CSB800°C, respectively.

2.3 Modification of Laver Biochar by Surfactant

2 g laver biochar and 1 g APG were mixed in 30 mL distilled water, transferred into a 50 mL Teflon reactor, and heated at 120°C for 24 h. After the reaction, the sample was filtered and dried to obtain sample A. 2 g sample A and 1 g RL were mixed in 30 mL distilled water and placed in a 50 mL Teflon reactor, heated at 120°C for 12 h. After that, the sample was filtered and dried to prepare surfactant-modified laver biochar. Surfactant modified CSB500°C, CSB600°C, CSB700°C and CSB800°C were denoted as MSAR500°C, MSAR600°C, MSAR700°C and MSAR800°C, respectively.

2.4 Characterization of As-Prepared Samples

The contact angle of the prepared samples was measured at 25°C using the sessile drop method (CA, XG-CAMB, Xuanyichuangxi Industrial Equipment, Shanghai, China). The crystal phase compositions of the samples were determined using an X-ray diffractometer (XRD, D/Max 2500, Agilent, USA). The diffraction peak intensity of the pieces at $2\theta = 20–50°$ was recorded at 40 kV and 30 mA. The functional groups of the samples were measured by Fourier transform infrared spectrometer (FTIR, Thermo Fisher Scientific, USA), and the chemical valence states of the samples were characterized by X-ray photoelectron spectroscopy (XPS, 5000C ESCA System, PHI, USA). The N_2 adsorption-desorption isotherm was performed on a specific surface area analyzer (Quadrasorb SI, Quantachrome, USA) and estimated with the method of Brunauer-Emmett-Teller (BET). The microstructure and morphology of the prepared biochars were analyzed by scanning electron microscopy (SEM, Hitachi S-4800, Tokyo, Japan). Elemental composition and distribution information were determined by energy-dispersive X-ray spectroscopy (EDS, Apollo XT, EDAX Company, USA). Transmission electron microscope (TEM; Tecnai G2 F20 S-TWIN (200KV), USA) was employed to analyze the morphology of the as-prepared sample. A Elementar Vario EL III was used to determine the elemental composition of carbon, hydrogen, nitrogen, oxygen, and sulfur. Raman Spectroscopy was performed in a Renishaw InVia Spectrometer (Renishaw, UK) with a 50x objective and equipped with a green laser line (532 nm).

2.5 Batch Adsorption Experiments

MSAR600°C was added into 50 mL of 1 g/L edible oil solution for adsorption experiments. The effects of initial pH, adsorption temperature, and adsorbent dose on the adsorption performances of edible oil were analyzed, respectively. Adjust the pH of the solution between 3.0 to 11.0 using 0.1 mol/L hydrochloric acid and 0.1 mol/L sodium hydroxide.

The adsorption temperature was controlled between 30°C to 70°C, and the dosage of the samples was from 0.005 to 0.025 g. After adsorption, the supernatant was taken at adsorption times of 10, 20, 30, 40, 50, 60, 90, and 120 min, centrifugated at 4000 r/min for 2 min, and extracted by n-hexane. The OD value of the

extracted solution was measured by UV-vis spectrophotometer (UV 2600, Shimadzu, Japan) at the maximum adsorption wavelength of 283 nm. Then OD value was used to calculate the concentration of edible oil (C_0 and C_e) in the adsorption system at different times.

The adsorption rate (R) and equilibrium adsorption capacity (q_e) of edible oil could be calculated according to the formula Eqs. (1) and (2), respectively.

$$R = \frac{C_0 - C_e}{C_0} \times 100\% \tag{1}$$

$$q_e = \frac{(C_0 - C_e)V}{m} \tag{2}$$

where R (%) is the adsorption rate of edible oil, q_e is the adsorption amount of edible oil at equilibrium, C_0 (mg/L) and C_e (mg/L) are edible oil concentration at the beginning and different time, respectively; and m (g) and V (L) are the mass of samples to added and the volume of edible oil solution, respectively.

2.6 Practical Application Experiments

0.5 g modified laver biochar mixed with 20 mL deionized water was used to prepare tableware detergent. Rapeseed oil and peanut oil were mixed well (v:v = 1:1), coated on a ceramic plate. Then dried the ceramic plate in an oven at 40°C for 20 min to cure the mixed oil. And the oil-coated ceramic plate was soaked in the as-prepared tableware detergent for 1 min, vibrated at a constant speed for 7 min with an oscillator, taken out, and dried. And the kitchen oil removal rate of modified laver biochar was determined by the gravimetric method and calculated according to Eq. (3). Moreover, the kitchen oil removal rate of the blank group without adding modified laver biochar and the commercial tableware detergent were also analyzed as the control.

$$D_r = \frac{M_1 - M_2}{M_1 - M_0} \times 100\% \tag{3}$$

where M_0 is the mass of the initial ceramic plate, M_1 is the mass of the oil-coated ceramic plate, and M_2 is the mass of the washed and dried ceramic plate.

2.7 Adsorption Kinetics Studies

In the kinetic experiments, 0.012 g of MSAR600°C and CSB600°C were added to 50 mL kitchen oil solutions, respectively. The edible oil concentration of the solution was measured at 30°C and at different adsorption times of 0–120 min. The adsorption kinetics of laver biochar and surfactant-modified hydrophobic biochar were analyzed by the pseudo-first-order (PFO) and pseudo-second-order kinetics (PSO) models, as follows Eqs. (4) and (5).

$$\ln(q_e - q_t) = lnq_e - k_1 t \tag{4}$$

$$\frac{t}{q_t} = \frac{1}{k_2 q_e^2} + \frac{t}{q_e} \tag{5}$$

where q_e (mg/g) is the amount of oil adsorption at the time (t), and k_1 (min^{-1}) and k_2 (g/mg min) are the rate parameters determined from the PFO and PSO models, respectively.

2.8 Standard Curve of Edible Oil

A small amount of n-hexane was used to dissolve 1 g of edible oil, which was mixed with 100 mL deionized water to obtain a 10 g/L edible oil standard reserve solution. 0.5, 1.0, 1.25, 1.5, 2.0, and 2.5 g/L edible oil solutions were prepared, respectively. The absorbance of edible oil solution in different

concentrations was measured at the maximum absorption wavelength of 214 nm. As shown in Fig. 1, the formula of the standard curve is y = 0.3074x – 0.0111, and the correlation coefficient R^2 = 0.9982.

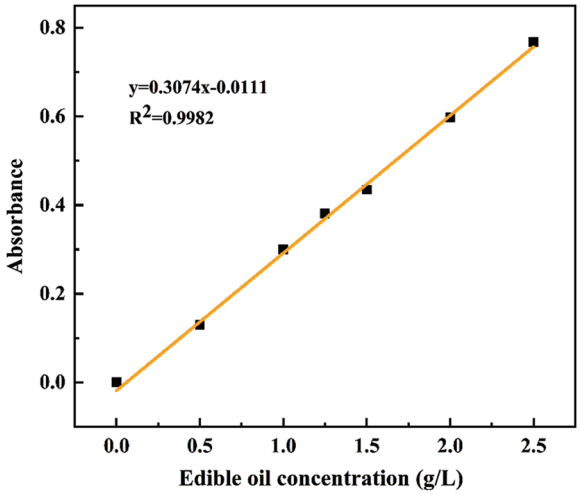

Figure 1: Standard curve for edible oil

3 Results and Discussion

3.1 Contact Angle Analysis

The contact angles of as-prepared modified laver biochar are shown in Fig. 2, and the contact angles of MSAR500°C, MSAR600°C, MSAR700°C and MSAR800°C are 135.1°, 137.5°, 135.6°, and 134.8°, respectively, which are all more than 90°, demonstrating that the surface of surfactant-modified laver biochar has excellent hydrophobicity. Among these, MSAR600°C has the utmost hydrophobic performance, whose contact angle is up to 137.5°. Algae biochar has abundant functional groups, especially polar hydroxy [26], with strong hydrophilicity. When its surface encounters a water droplet, it is absorbed immediately, so it is impossible to measure the contact angle of laver biochar. APG, a nonionic surfactant, modified the laver biochar, whose hydrophilic head attached to the hydroxyl groups of laver biochar, exposing its hydrophobic tail. Then the laver biochar was further modified with anionic surfactant RL to enhance its hydrophobicity and dispersion stability. Considering the hydrophobic performance and energy consumption, MSAR600°C was selected as the best adsorbent for the subsequent kitchen oil removal experiment.

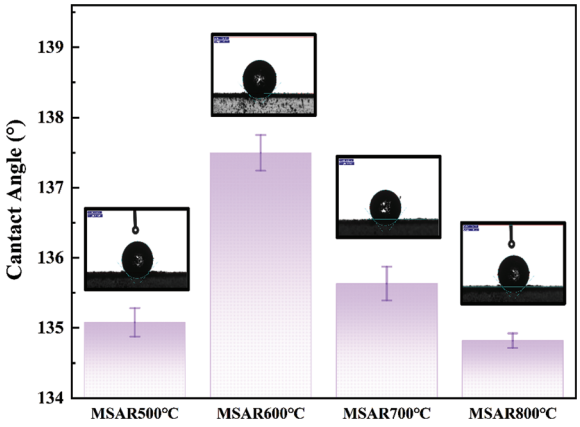

Figure 2: Water contact angle values of modified laver biochar

3.2 Morphology Analysis

Table 1 shows the specific surface area and average pore size of laver biochar at different calcination temperatures (CSB500°C, CSB600°C, CSB700°C, CSB800°C) and modified laver biochar (MSAR600°C). It can be observed that CSB600°C has the largest specific surface area, up to 7.86 m^2/g, after surfactant modification, whose specific surface area increases by 3 times, up to 23.4 m^2/g, while whose average pore size has no significant change, indicating that surfactants increase its specific surface area by improving its dispersibility. When the calcination temperature exceeds 600°C, the specific surface area of laver biochar decreases gradually, and it is speculated that the pore size collapse of biochar leads to the decrease of the surface area.

Table 1: Specific surface area and average pore size of laver biochar and modified laver biochar

Different materials	Specific surface area (m^2/g)	Average pore size (nm)
CSB500°C	7.02	2.38
CSB600°C	7.86	1.67
CSB700°C	4.26	3.93
CSB800°C	3.32	3.93
MSAR600°C	23.4	1.74

According to IUPAC classification [30], it has been found that the N_2 adsorption isotherms of CSB600°C and MSAR600°C are all type IV, as shown in Fig. 3. When the relative pressure (P/P_0) is between 0.1 and 1.0, type H3 hysteresis regression line appears, indicating the presence of mesopores. And it can be demonstrated from the pore size distribution curve that the pore diameter of CSB600°C is mostly between 0 and 10 nm; after modification, the pore diameter of MSAR600°C is in the range of 0–50 nm. Therefore, APG and RL modification could enlarge the aperture distribution range of laver biochar, render MSAR600°C hierarchical porous structure, and it is beneficial to the adsorption of oil molecules.

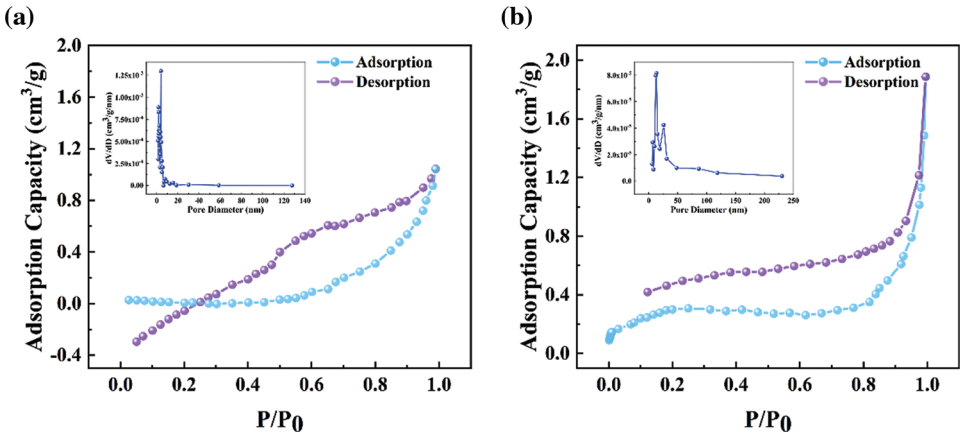

Figure 3: N_2 adsorption-desorption isotherm and pore size distribution of CSB600°C (a) and MSAR600°C (b)

SEM images of CSB600°C and MSAR600°C at different magnifications are shown in Figs. 4a–4b. CSB600°C exhibits a relatively smooth layered structure with cracks and debris, while MSAR600°C exhibits a periodic concave-convex and wave-like structure. As is well known, the surface of lotus leaves has droplet contact angles of over 150°, with super hydrophobicity, which is brought about by the micro/nano-scale papillae structures on the leaf surface and the layer of wax crystals on these structures [31]. After surfactant modification, laver biochar possesses a louts-leaf-like papillae microstructure, endowing its high specific surface area and hydrophobic performance, consistent with contact angle and BET results. The microstructure, size, lattice streaks, and exposed crystal planes of the as-prepared samples can be analyzed by TEM and HRTEM, as shown in Figs. 4e and 4f. It can be observed that CSB600°C behaves as a typical amorphous material characteristic in Fig. 4e, having no apparent lattice structure. After APG and RL modification, MSAR600°C exhibits the lattice structure, and two lattices spacing 0.349 and 0.284 nm are observed, corresponding to the (020) surface and (012) surface of $CaSO_4$, respectively.

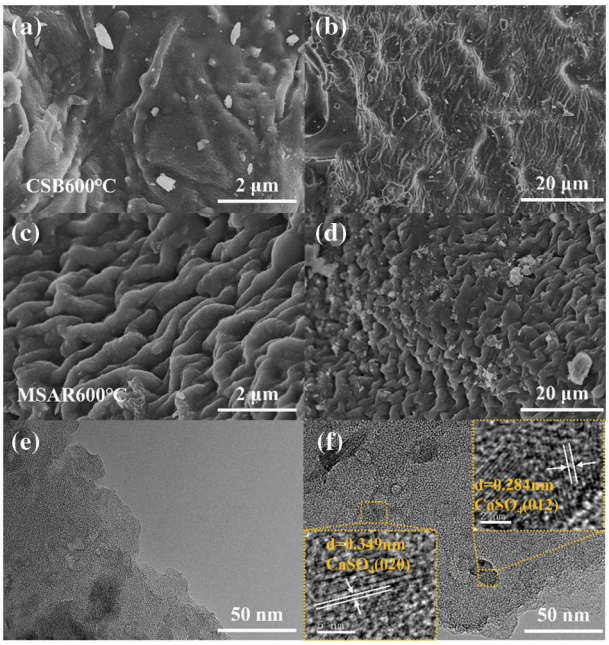

Figure 4: SEM images of CSB600°C and MSAR600°C: (a, b) CSB600°C; (c, d) MSAR600°C; the TEM images of CSB600°C and MSAR600°C, (e) the TEM of CSB600°C; (f) the TEM of MSAR600°C

3.3 Chemical Composition Analysis

To determine the crystal phase of laver biochar before and after modification, XRD characterization was carried out, as shown in Fig. 5a. It can be observed that the diffraction peaks of $2\theta = 25.4°$, 31.4° and 38.6° in the spectrum of CSB600°C correspond to the (020), (012) and (022) crystal planes of $CaSO_4$ (JCPDS card No. 80-0787), respectively. The diffraction peaks at MSAR600°C are 2θ = 31.4° and 44.9°, which correspond to the (200) and (220) crystal planes of CaS (PDF card No. 77-2011), respectively. Laver is a kind of red algae, rich in calcium alginate and various amino acids, especially sulfur amino acids [28], which were decomposed and reacted to form $CaSO_4$ at high-temperature carbonization. Then $CaSO_4$ was further degraded into CaS under the reducing reaction of RL. Fig. 5b shows the FTIR spectra of CSB600°C and MSAR600°C. It can be seen that the infrared absorption peaks of laver biochar before and after modification are basically the same. The relatively wide absorption peaks at 3428 and

3431 cm^{-1} are the stretching vibration of the hydroxyl group (-OH) in alcohols, phenols, and carboxylic acids. And the adsorption peak at 1583 and 1586 cm^{-1} are the stretching vibrations of C=O, and the adsorption peaks at 1109 and 588 cm^{-1} of MSAR600°C and those at 1109 and 572 cm^{-1} of CSB600°C are characteristic peaks of $CaSO_4$, which is consistent with XRD results.

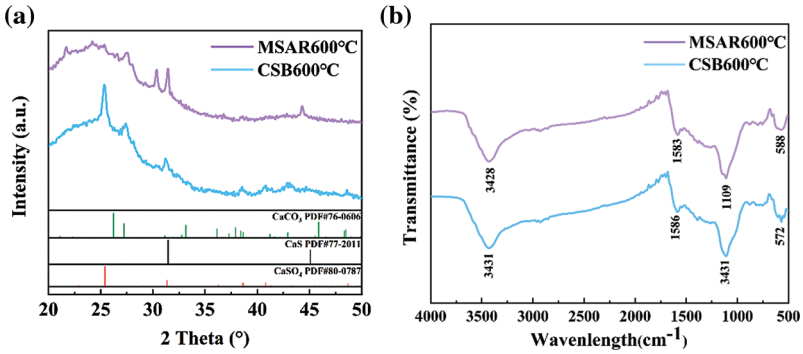

Figure 5: XRD patterns (a) and FTIR spectra (b) of CSB600°C and MSAR600°C

Elemental analysis was employed to clarify the element composition of the CSB600°C and MSAR600°C, as shown in Table 2. It can be seen that the content of C, H, N, O, and S nonmetallic elements does not change significantly in CSB600°C and MSAR600°C. This indicated that the surfactant modification did not change the elemental composition of laver biochar. And C content of CSB600°C and MSAR600°C are maximum, up to 66.687% and 67.693%, respectively, followed by O, N, S, and H. Typically, the O/C atomic ratio manifests the hydrophobicity of biochar, and estimated the aromaticity of biochar by H/C atomic ratio [32]. And the lower the polarity, the higher the aromaticity, and the greater the hydrophobicity [33].

Table 2: Element analysis of CSB600°C and MSAR600°C (%)

	C	H	O	N	S	O/C	H/C
CSB600°C	66.687	2.325	14.509	6.117	2.423	0.218	0.035
MSAR600°C	67.693	2.266	13.425	6.217	2.355	0.198	0.033

After surfactant modification, the O/C and H/C ratios of MSAR600°C are lower (0.198, 0.033) than those of CSB600°C (0.218, 0.035), manifesting that MSAR600°C has higher hydrophobicity, being consistent with the results of contact angle.

EDS-mapping was used to further explore the surface elemental composition of as-prepared samples before and after modification, as exhibited in Figs. 6a–6l. It can be indicated that the contents of C, N, and O have no significant change in CSB600°C and MSAR600°C (Table 3), while Ca and S are concentrated in the region covered by the surfactant in MSAR600°C, whose content significantly improve compared with those in CSB600°C, indicating that APG and RL react with CSB 600°C to form a new substance containing calcium and sulfur, i.e., CaS, consisting with the results of XRD. The distribution of C and O are relatively homogeneous in CSB600°C, while C and O are concentrated in the region without surfactant in MSAR600°C, indicating that APG and RL were successfully loaded on the surface of CSB600°C.

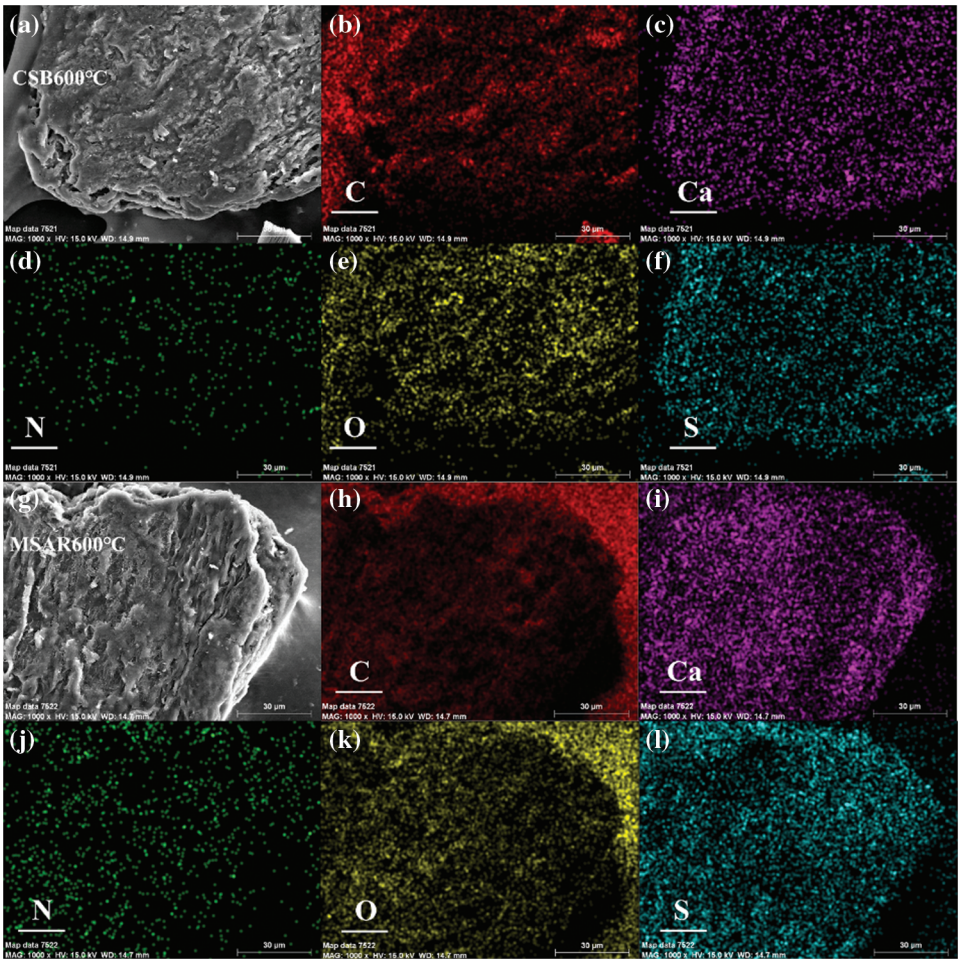

Figure 6: The EDS mapping images of CSB600°C (a–f) and MSAR600°C (g–l)

Table 3: The EDS quantitative analysis results of CSB600°C and MSAR600°C

Element	CSB600°C		MSAR600°C	
	Weight%	Atomic%	Weight%	Atomic%
C	71.05	77.31	66.93	75.46
N	7.74	7.22	7.75	7.49
O	17.07	13.95	16.24	13.75
S	2.14	0.87	2.69	1.14
Ca	2.00	0.65	6.40	2.16

XPS was performed to determine the elemental composition and chemical states of as-prepared samples, as shown in Fig. 7. It can be observed from Fig. 7a that CSB600°C and MSAR600°C contain C, N, and O elements, and the binding energies of C1s, N1s and O1s are 284.7, 400.2 and 532.2 eV, respectively. And the peaks in the C1s spectrum of CSB600°C with the relevant binding energies of 287.68, 286.18, and 284.78 eV, correspond to C=O, C-O, and C-C, respectively. And the peaks in the C 1s spectrum of

MSAR600°C with the relevant binding energies of 288.38, 286.18, and 284.55 eV correspond to C=O, C-O, and C-C. Therefore, laver biochar is rich in various oxygen-containing functional groups, providing active sites for kitchen oil adsorption, which is consistent with FTIR results.

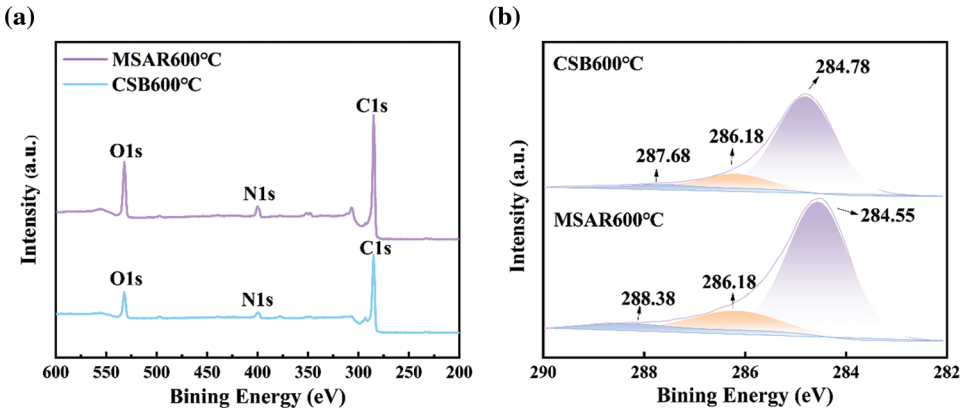

Figure 7: XPS spectra of the CSB600°C and MSAR600°C: (a) full spectrum, (b) carbon spectrum

Raman spectroscopy was employed to investigate the lattice disorder of as-prepared samples, as shown in Fig. 8. The G band (1580 cm^{-1}), generally generated by the symmetric stretching vibration of the benzene ring in the crystalline graphite carbon and the stretching vibration of the C=C bond conjugated with the benzene ring, that is, all the sp2 vibrations in the carbon ring or long chain. While the D band (1350 cm^{-1}) is mainly caused by graphite lattice defects. The intensity ratio of the D band and G band (I_D/I_G) was regarded as an indicator of defective degree [34]. It can be observed that the defective degree (I_D/I_G) of laver biochar decreased from 1.1063 to 1.0802 after surfactant modification, indicating that APG and RL might be covering the intrinsic defects of laver biochar, giving rise to the decrease of lattice defects, disordered edge arrangements and low symmetry-structure carbon, and the increase of disorder in MSAR600°C.

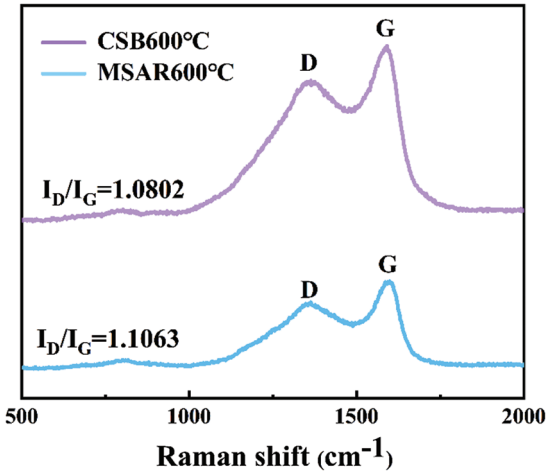

Figure 8: Raman analysis of CSB600°C and MSAR600°C

3.4 Batch Adsorption Experiments

3.4.1 Effect of Adsorption Time

The effect of adsorption time on kitchen oil using CSB600°C and MSAR600°C was analyzed, as shown in Fig. 9a. It could be revealed that MSAR600°C has a higher adsorption capacity for kitchen oil than CSB600°C, which is mainly due to the porous structure of laver biochar and enhanced hydrophobic performance after modification by APG and RL.

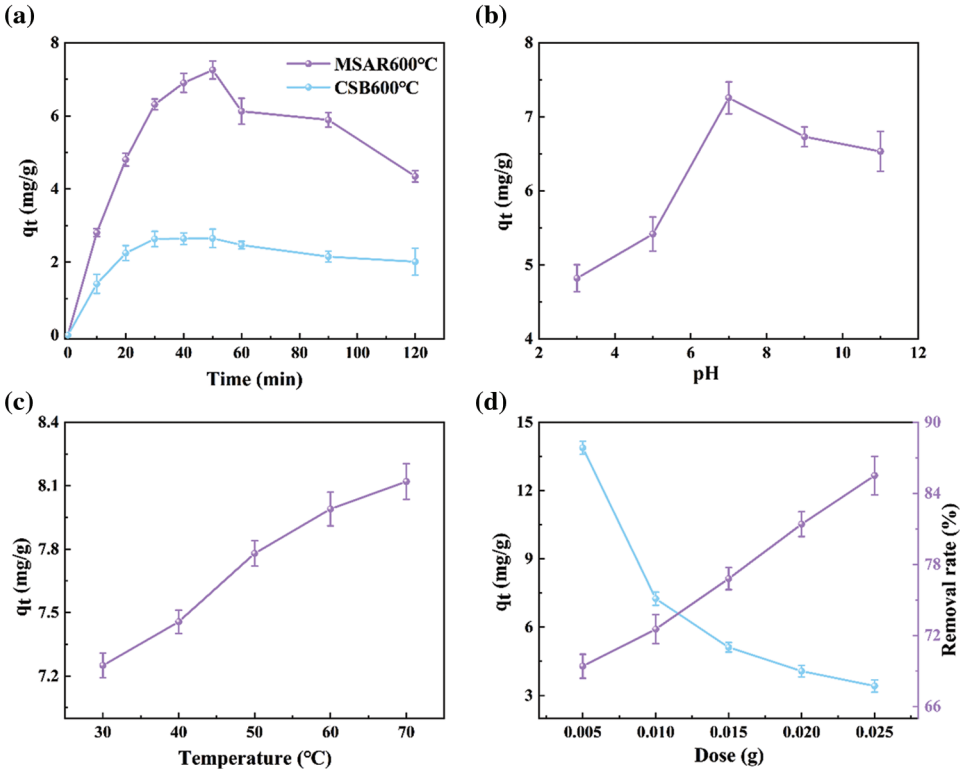

Figure 9: Effects of adsorption time (a), pH (b), temperature (c), and adsorbent dose (d) on kitchen oil adsorption using MSAR600°C

Therefore, MSAR600°C exhibits superior adsorption performance for the kitchen oil; when the adsorption time is 50 min, the maximum adsorption capacity can reach 7.253 mg/g. It can be observed that the adsorption amount of kitchen oil using MSAR600°C shows an upward trend in the first 50 min, mainly due to its high hydrophobicity, which can quickly bind oil molecules based on the principle of the dissolution in a similar material structure. And the adsorption amount showed a gentle downward trend in 50–120 min, ascribed to the abundant porous structure having superior liquid diffusion performance, which is conducive to the adsorption of oil molecules. Therefore, in further adsorption experiments, the optimal adsorption time is 50 min.

3.4.2 Effect of pH

Generally, pH plays an important role in adsorption, the solution pH determines the kind of interaction between the adsorbent and kitchen oil through the ionization of species in the solution. Fig. 9b shows the effect of pH on kitchen oil adsorption using MSAR600°C between 3.0 to 11.0. It can be demonstrated that the adsorption capacity of kitchen oil increases at first and then decreases as the pH goes up.

Therefore, the optimum pH for kitchen oil removal is 7, which will be used for the subsequent experiments. RL is an anionic surfactant whose activity is easily destroyed under acidic conditions [35], while APG is a nonionic surfactant whose activity is unaffected by pH [36]. Thus, the adsorption capacity of kitchen oil using MSAR600°C is lower under the acidic condition, while that is higher under the neutral and alkaline conditions.

3.4.3 Effect of Adsorption Temperature

Temperature plays a vital role in the adsorption of kitchen oil by MSAR600°C. Fig. 9c shows that in the range of 30°C to 70°C, the adsorption capacity increases with adsorption temperature. The surface activity of APG and RL are not affected by the adsorption temperature in the range of 30°C to 70°C, while the increase of temperature improves the diffusion performance of oil pollution molecules and enhances the adsorption efficiency of kitchen oil.

3.4.4 Effect of Absorbent Dose

Fig. 9d shows the adsorption performance for kitchen oil at different doses of MSAR600°C. The unit adsorption capacity for kitchen oil using MSAR600°C declined sharply and leveled off gradually, when increasing absorbent dose in the range of 0.005–0.025 g, while the removal rate straight up. This is due to the increase of the adsorbent dose. The number of active sites on the surface of the adsorbent increased, which can absorb more oil molecules and then lead to a rapid increase in removal rate. However, with the increase of the adsorbent dose, the oil adsorption cannot reach saturation, resulting in a gradual decrease in the unit adsorption capacity. Considering the unit adsorption capacity and removal rate, the adsorbent dose is 0.012 g in the follow-up experiment.

3.4.5 Adsorption Kinetics Study

The adsorption kinetics of MSAR600°C and CSB600°C for the kitchen oil are investigated using PFO (Fig. 10a) and PSO (Fig. 10b) models. The adsorption kinetic parameters of MSAR600°C and CSB600°C for edible oil are shown in Table 4. It can be seen that the R^2 value of the PFO model for edible oil is higher than that of the PSO model. This indicates that MSAR600°C and CSB600°C are mainly physical adsorptions, involving pore filling and Van der Waals force or electrostatic force [37]. This may be due to the presence of surfactants, the oil molecules, and the surfactant on the material's surface between the Van der Waals force. At the same time, the pore size structure of the material surface provides active sites for oil molecules [38]. The materials cannot hold oil molecules for long [19,39].

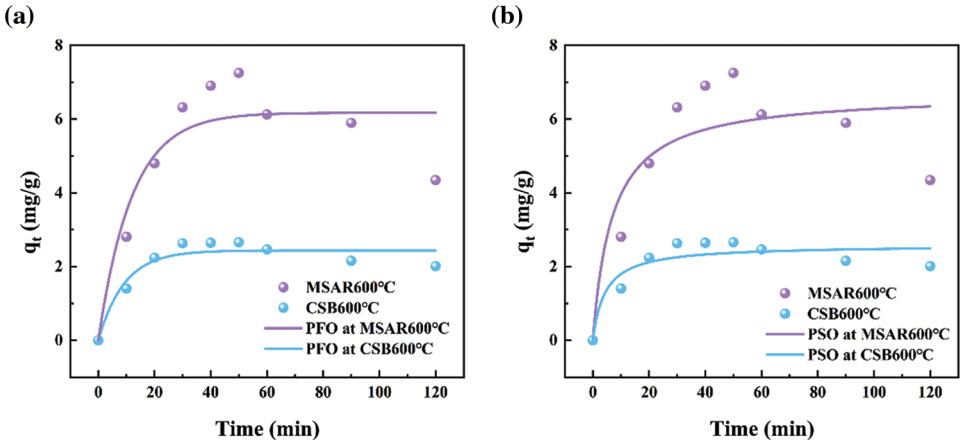

Figure 10: MSAR600°C and CSB600°C adsorption kinetics of kitchen oil: (a) pseudo first order model (b) pseudo second order model

Table 4: The adsorption kinetic parameters for kitchen oil adsorption using MSAR600°C and CSB600°C

Sample	Pseudo-first-order			Pseudo-second-order		
	q_e (mg/g)	k_1 (min^{-1})	R_1^2	q_e (mg/g)	k_2 (g/mg min)	R_2^2
MSAR600°C	6.173	0.083	0.84492	6.713	0.021	0.746
CSB600°C	2.439	0.108	0.91442	2.584	0.088	0.861

3.5 Kitchen Oil Removal Efficiency

The laver biochar at different calcination temperatures and surfactant-modified biochar were tested for the removal of kitchen oil, as shown in Fig. 11. It can be demonstrated that the removal rate of CSB500°C, CSB600°C, CSB700°C, CSB800°C, and MSAR600°C is 25.14%, 43.34%, 32.84%, 25.26%, and 75.98%, respectively. Thus, the laver biochar with surfactant modification has higher removal efficiency of kitchen oil, and MSAR600°C has the maximum removal rate, up to 75.98%. Meanwhile, the kitchen oil removal rate of a commercial tableware detergent (CAD) was measured for comparison, up to 72.3%, less than that of MSAR600°C (75.98%). It can be demonstrated that MSAR600°C possesses a larger specific surface area and higher hydrophobicity from BET results and contact angle, being beneficial to the adsorption of kitchen oil molecules.

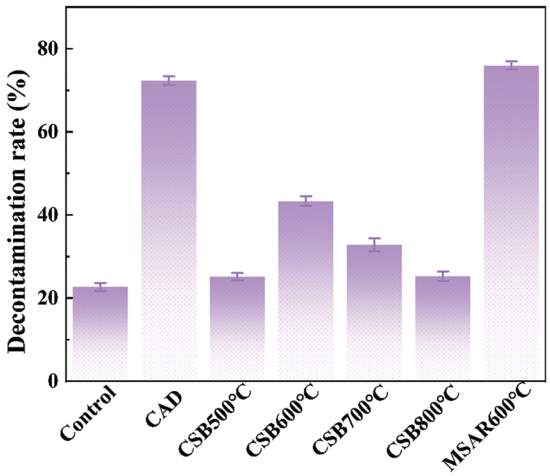

Figure 11: Oil removal rate of laver biochar before and after modification

3.6 Kitchen Oil Removal Mechanism

As we all know, the principle of oil removal is the comprehensive embodiment of infiltration, emulsification and dispersion, and solubility. In Fig. 12, the hydrophilic group and the hydrophobic group in the surfactant are adsorbed on the interface between oil and solution; the hydrophilic group points to the solution and the hydrophobic group points to the oil, directional arrangement, so that the oil-liquid interfacial tension is greatly reduced. Under the stirring action, the oil is loose, easy to disperse into tiny oil beads and separated from the workpiece surface. And surfactants aids through emulsification and dispersion; the oil beads cannot merge and re-adhere to the workpiece surface to achieve the cleaning effect. Researchers have developed various biochar for the application of oil pollution treatment due to their rich pore structure, high specific surface area, and a variety of oxygen-containing functional groups

[5,40,41]. However, the surface of biochar contains many hydrophilic groups, such as -OH, which is not conducive to the efficient adsorption of oil molecules. Therefore, two environmentally friendly surfactants, APG and RL, were used to modify laver biochar (CSB). The hydrophilic groups of the surfactants were linked to the hydrophilic groups on the surface of the CSB, so that more hydrophobic groups were exposed on the surface, which could efficiently adsorb kitchen oil. At the same time, the surfactant can reduce the surface energy of biochar, increase the dispersion, improve the contact efficiency of biochar and oil, and further improve oil adsorption. In addition, the surface of modified laver biochar (MSAR) shows a porous structure and high specific surface area, which can also achieve efficient oil adsorption. The MSAR adsorbed oil is washed with water and emulsified with surfactants to attain efficient oil removal.

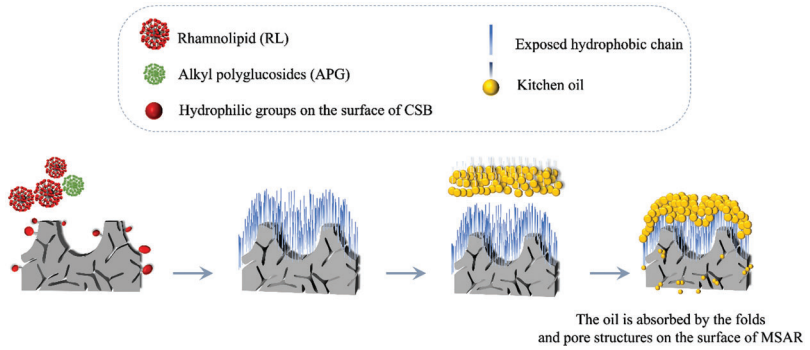

Figure 12: The mechanism of cleaning materials to remove cooking oil

4 Conclusion

In this paper, a novel tableware detergent was developed from a macroalga, laver (*Porphyra haitanensis*), which was high-temperature carbonized, and modified with APG and RL surfactants, endowing it with porous structure and hydrophobic surface properties. After surfactant modification, MSAR600°C exhibits a louts-leaf-like papillae microstructure, endowing its high specific surface area (23.4 m^2/g), hydrophobic performance (Contact angle is 137.5°), and various oxygen-containing functional groups (-OH, C=O, C-O), being beneficial to the adsorption of oil molecules. The removal rate of kitchen oil using MSAR600°C is as high as 75.98%, which is even better than that using commercial detergent (72.3%), mainly because MSAR600°C contains large specific surface area, abundant porous structure, and various oxygen-containing functional groups, providing more adsorption sites for oil molecules. In addition, APG and RL grant laver biochar higher hydrophobic, dispersive and emulsifying properties, which further improve the oil removal efficiency. Therefore, the tableware detergent prepared from laver in this work exhibits comprehensive materials source, low cost, high efficiency, and environmental friendliness, and the enormous application potential in green tableware detergent.

Funding Statement: This study was supported by the Fundamental Research Funds for Zhejiang Provincial Universities and Research Institutes (No. 2021J004) and the Scientific Research Fund of Zhejiang Provincial Education Department (No. Y202044721).

Conflicts of Interest: The authors declare that they have no conflicts of interest to report regarding the present study.

References

1. Dai, M., Guo, J., Xue, X., Feng, Y. (2019). Preparation and investigation of high-efficiency antibacterial liquid dishwashing detergent. *Transactions of Tianjin University, 25(4),* 322–329. https://doi.org/10.1007/s12209-019-00187-x

2. Klimantova, V., Raclavska, H., Bouchalova, J. (2020). Dishwashing detergents and their effects on respiration inhibition of activated sludge. *IOP Conference Series: Earth and Environmental Science, 444(1),* 012026. https://doi.org/10.1088/1755-1315/444/1/012026
3. Wu, H. Y., Shih, C. L., Lee, T., Chen, T. Y., Lin, L. C. et al. (2019). Development and validation of an analytical procedure for quantitation of surfactants in dishwashing detergents using ultra-performance liquid chromatography-mass spectrometry. *Talanta, 194,* 778–785. https://doi.org/10.1016/j.talanta.2018.10.084
4. Yang, Y., Jiang, X., Goh, K. L., Wang, K. (2021). The separation of oily water using low-cost natural materials: Review and development. *Chemosphere, 285,* 131398. https://doi.org/10.1016/j.chemosphere.2021.131398
5. Madhubashani, A. M. P., Giannakoudakis, D. A., Amarasinghe, B., Rajapaksha, A. U., Pradeep Kumara, P. B. T. et al. (2021). Propensity and appraisal of biochar performance in removal of oil spills: A comprehensive review. *Environmental Pollution, 288,* 117676. https://doi.org/10.1016/j.envpol.2021.117676
6. Bandura, L., Woszuk, A., Kołodyńska, D., Franus, W. (2017). Application of mineral sorbents for removal of petroleum substances: A review. *Minerals, 7(3),* 37. https://doi.org/10.3390/min7030037
7. Kumagai, S., Noguchi, Y., Kurimoto, Y., Takeda, K. (2007). Oil adsorbent produced by the carbonization of rice husks. *Waste Management, 27(4),* 554–561. https://doi.org/10.1016/j.wasman.2006.04.006
8. Swaren, L., Safari, S., Konhauser, K. O., Alessi, D. S. (2022). Pyrolyzed biomass-derived nanoparticles: A review of surface chemistry, contaminant mobility, and future research avenues to fill the gaps. *Biochar, 4(1),* 33. https://doi.org/10.1007/s42773-022-00152-3
9. Ma, J., Huang, W., Zhang, X., Li, Y., Wang, N. (2021). The utilization of lobster shell to prepare low-cost biochar for high-efficient removal of copper and cadmium from aqueous: Sorption properties and mechanisms. *Journal of Environmental Chemical Engineering, 9(1),* 104703. https://doi.org/10.1016/j.jece.2020.104703
10. Vithanage, M., Herath, I., Joseph, S., Bundschuh, J., Bolan, N. S. et al. (2017). Interaction of arsenic with biochar in soil and water: A critical review. *Carbon, 113(1),* 219–230. https://doi.org/10.1016/j.carbon.2016.11.032
11. Zhu, B., Liu, B., Qu, C., Zhang, H., Guo, W. et al. (2018). Tailoring biomass-derived carbon for high-performance supercapacitors from controllably cultivated algae microspheres. *ChemElectroChem, 6(2),* 1523–1530. https://doi.org/10.1002/celc.201300127
12. Guirado, M., Garrido-Sanz, D., Pindado, O., Rodríguez-Rastrero, M., Merino-Martín, L. et al. (2021). Effectiveness of biochar application and bioaugmentation techniques for the remediation of freshly and aged diesel-polluted soils. *International Biodeterioration & Biodegradation, 163,* 105259. https://doi.org/10.1016/j.ibiod.2021.105259
13. Saeed, M., Ilyas, N., Jayachandran, K., Gaffar, S., Arshad, M. N. et al. (2021). Biostimulation potential of biochar for remediating the crude oil contaminated soil and plant growth. *Saudi Journal of Biological Sciences, 28(5),* 2667–2676. https://doi.org/10.1016/j.sjbs.2021.03.044
14. Russell, T. P. (2002). Surface-responsive materials. *Science, 297(5583),* 964–967. https://doi.org/10.1126/science.1075997
15. Sun, Q., Chen, M., Aguila, B., Nguyen, N., Ma, S. (2017). Enhancing the biofuel upgrade performance for Pd nanoparticles via increasing the support hydrophilicity of metal-organic frameworks. *Faraday Discussions, 201,* 317–326. https://doi.org/10.1039/C7FD00015D
16. Li, Y., Zhao, C. (2017). Enhancing water oxidation catalysis on a synergistic phosphorylated NiFe hydroxide by adjusting catalyst wettability. *ACS Catalysis, 7(4),* 2535–2541. https://doi.org/10.1021/acscatal.6b03497
17. Klimov, V. V., Bryuzgin, E. V., Le, M. D., Zelenova, E. A., Nguyen, T. H. et al. (2016). An investigation of the hydrophobic property stability of grafted polymeric coatings on a cellulose material surface. *Polymer Science Series D, 9(4),* 364–367. https://doi.org/10.1134/S1995421216040080
18. Zhou, J., Guo, J., Yan, H., Xiao, J., Wang, J. (2021). Reversible wettability switching of melamine sponges for oil/water separation. *Materials Chemistry and Physics, 257(19),* 123772. https://doi.org/10.1016/j.matchemphys.2020.123772
19. Bianco, F., Marcińczyk, M., Race, M., Papirio, S., Esposito, G. et al. (2022). Low temperature-produced and VFA-coated biochar enhances phenanthrene adsorption and mitigates toxicity in marine sediments. *Separation and Purification Technology, 296,* 121414. https://doi.org/10.1016/j.seppur.2022.121414

20. AlAmeri, K., Giwa, A., Yousef, L. F., Alraeesi, A., Taher, H. (2019). Sorption and removal of crude oil spills from seawater using peat-derived biochar: An optimization study. *Journal of Environmental Management, 250(1),* 109465. https://doi.org/10.1016/j.jenvman.2019.109465
21. Sidik, S. M., Jalil, A. A., Triwahyono, S., Adam, S. H., Satar, M. A. H. et al. (2012). Modified oil palm leaves adsorbent with enhanced hydrophobicity for crude oil removal. *Chemical Engineering Journal, 203,* 9–18. https://doi.org/10.1016/j.cej.2012.06.132
22. Navarathna, C. M., Bombuwala Dewage, N., Keeton, C., Pennisson, J., Henderson, R. et al. (2020). Biochar adsorbents with enhanced hydrophobicity for oil spill removal. *ACS Applied Materials & Interfaces, 12(8),* 9248–9260. https://doi.org/10.1021/acsami.9b20924
23. Gurav, R., Bhatia, S. K., Choi, T. R., Choi, Y. K., Kim, H. J. et al. (2021). Adsorptive removal of crude petroleum oil from water using floating pinewood biochar decorated with coconut oil-derived fatty acids. *Science of the Total Environment, 781,* 146636. https://doi.org/10.1016/j.scitotenv.2021.146636
24. Wei, D., Zhang, H., Cai, L., Guo, J., Wang, Y. et al. (2018). Calcined mussel shell powder (CMSP) via Modification with Surfactants: Application for antistatic oil-removal. *Materials, 11(8),* 1410–1423. https://doi.org/10.3390/ma11081410
25. Yang, Y., Wu, Z., Ji, L., Lu, S., Jing, H. et al. (2021). Preparation of porous materials derived from waste mussel shell with high removal performance for tableware oil. *Journal of Renewable Materials, 9(11),* 1869–1881. https://doi.org/10.32604/jrm.2021.015952
26. Jiang, X., Wang, H., Hu, E. M, Lei, Z., Fan, B. et al. (2020). Efficient adsorption of uranium from aqueous solutions by microalgae based aerogel. *Microporous and Mesoporous Materials, 305(3),* 110383. https://doi.org/10.1016/j.micromeso.2020.110383
27. Du, Y., Hayashi, S., Shen, S. L. (2014). Impact of laver treatment practices on the geoenvironmental properties of sediments in the Ariake Sea. *Marine Pollution Bulletin, 81(1),* 41–48. https://doi.org/10.1016/j.marpolbul.2014.02.027
28. Hwang, E. S., Ki, K. N., Chung, H. Y. (2013). Proximate composition, amino acid, mineral, and heavy metal content of dried laver. *Preventive Nutrition and Food Science, 18(2),* 139–144. https://doi.org/10.3746/pnf.2013.18.2.139
29. Pan, C., Ma, J., Tao, F., Ji, C., Zhao, Y. et al. (2021). Novel insight into the antioxidant proteins derived from laver (*Porphyra haitanensis*) by proteomics analysis and protein based bioinformatics. *Food Bioscience, 42,* 101134. https://doi.org/10.1016/j.fbio.2021.101134
30. Sing, K. S. W. (1985). Reporting physisorption data for gas/solid systems with special reference to the determination of surface area and porosity. *Pure and Applied Chemistry, 57(4),* 603–619. https://doi.org/10.1351/pac198557040603
31. Hao, P., Yao, Z., Zhang, X. (2011). Study of dynamic hydrophobicity of micro-structured hydrophobic surfaces and lotus leaves. *Science China Physics, Mechanics and Astronomy, 54(4),* 675–682. https://doi.org/10.1007/s11433-011-4269-1
32. Yao, X., Ji, L., Guo, J., Ge, S., Lu, W. et al. (2020). An abundant porous biochar material derived from wakame (*Undaria pinnatifida*) with high adsorption performance for three organic dyes. *Bioresource Technology, 318(1),* 124082. https://doi.org/10.1016/j.biortech.2020.124082
33. Shen, Z., Zhang, Y., McMillan, O., O'Connor, D., Hou, D. (2020). *The use of biochar for sustainable treatment of contaminated soils*. Butterworth-Heinemann Location: Butterworth-Heinemann.
34. He, X., Zheng, N., Hu, R., Hu, Z., Yu, J. C. (2020). Hydrothermal and pyrolytic conversion of biomasses into catalysts for advanced oxidation treatments. *Advanced Functional Materials, 31(7),* 2006505. https://doi.org/10.1002/adfm.202006505
35. Khan, M. B., Sasmal, C. (2022). A detailed and systematic study on rheological and physicochemical properties of rhamnolipid biosurfactant solutions. *JCIS Open, 8(11),* 100067. https://doi.org/10.1016/j.jciso.2022.100067
36. Aslam, R., Mobin, M., Aslam, J., Aslam, A., Zehra, S. et al. (2021). Application of surfactants as anticorrosive materials: A comprehensive review. *Advances in Colloid and Interface Science*, *295*. https://doi.org/10.1016/j.cis.2021.102481

37. Braghiroli, F. L., Bouafif, H., Neculita, C. M., Koubaa, A. (2019). Performance of physically and chemically activated biochars in copper removal from contaminated mine effluents. *Water, Air, & Soil Pollution, 230(8),* 178. https://doi.org/10.1007/s11270-019-4233-7

38. Park, J., Hung, I., Zhehong, G., Rojas, O. J., Lim, K. H. et al. (2013). Activated carbon from biochar: Influence of its physicochemical properties on the sorption characteristics of phenanthrene. *Bioresource Technology, 149,* 383–398. https://doi.org/10.1016/j.biortech.2013.09.085

39. Bianco, F., Race, M., Papirio, S., Oleszczuk, P., Esposito, G. (2022). Coupling of desorption of phenanthrene from marine sediments and biodegradation of the sediment washing solution in a novel biochar immobilized-cell reactor. *Environmental Pollution, 308,* 119621. https://doi.org/10.1016/j.envpol.2022.119621

40. Singh, R., Dutta, R. K., Naik, D. V., Ray, A., Kanaujia, P. K. (2021). High surface area Eucalyptus wood biochar for the removal of phenol from petroleum refinery wastewater. *Environmental Challenges, 5(7),* 100353. https://doi.org/10.1016/j.envc.2021.100353

41. Wang, Q., Deng, J., Liang, J., Jiang, L. Y, Arslan, M. et al. (2019). Biochar immobilized petroleum degrading consortium for enhanced granulation and treatment of synthetic oil refinery wastewater. *Bioresource Technology Reports, 17(1),* 100909. https://doi.org/10.1016/j.biteb.2021.100909